Effects of boundary conditions and gradient flow in 1+1 dimensional lattice ϕ^4 theory

A. Harindranath[1,*] and Jyotirmoy Maiti[2,†]

[1] *Theory Division, Saha Institute of Nuclear Physics 1/AF Bidhan Nagar, Kolkata 700064, India*

[2] *Department of Physics, Tehatta Government College, Tehatta, Nadia, West Bengal 741160, India*

(Dated: January 17, 2017)

In this work we study the effects of gradient flow and open boundary condition in the temporal direction in 1+1 dimensional lattice ϕ^4 theory. Simulations are performed with periodic (PBC) and open (OPEN) boundary conditions in the temporal direction. The Effects of gradient flow and open boundary on the field ϕ and the susceptibility are studied in detail along with the finite size scaling analysis. In both cases, at a given volume, the phase transition point is shifted towards a lower value of lattice coupling λ_0 for fixed m_0^2 in the case of OPEN as compared to PBC with this shift found to be diminishing as volume increases. We compare and contrast the extraction of the boson mass from the two point function (PBC) and the one point function (OPEN) as the coupling, starting from moderate values, approaches the critical value corresponding to the vanishing of the mass gap. In the critical region, boundary artifacts become dominant in the latter. Our studies point towards the need for a detailed finite volume (scaling) analysis of the effects of OPEN in the critical region.

arXiv:1701.04601v1 [hep-lat] 17 Jan 2017

* a.harindranath@saha.ac.in

† jyotirmoy.maiti@gmail.com

I. INTRODUCTION AND MOTIVATION

The quantum field theory of 1+1 dimensional ϕ^4 interaction, in spite of its apparent simplicity, has a very rich structure and hence has been the testing ground for various new non-perturbative approaches towards the field theory. It also provides ample opportunity to study newly proposed algorithms and calculational techniques. Extensive numerical results have been presented in this theory in an earlier work [1]. In this work we present numerical studies in this theory in the context of comparison between periodic (PBC) and open boundary conditions (OPEN) in the temporal direction and the effects of gradient flow (also known as Wilson flow).

In addition to the periodic boundary conditions in both temporal and spatial directions, one can have other types of boundary conditions. For the scalar field, for example, one can have anti-periodic boundary condition in the spatial direction (APBC). In the latter case one can study quantum kinks [2]. Lattice Quantum ChromoDynamics (LQCD) conventionally uses PBC in both the temporal and spatial directions for the gauge field. However, in this case, the spanning of gauge configurations over different topological sectors becomes more and more difficult as the continuum limit is approached. As a remedy, open boundary condition in the temporal direction has been proposed [3–5]. Numerical studies in pure Yang-Mills theory [6–10] and QCD [11] have yielded encouraging results.

In order for OPEN to be effective, boundary artifacts should be negligible so that one has a bulk region of considerable extent. This is possible as long the system is not gap less (critical) [12]. The success of OPEN in pure Yang-Mills theory and QCD hinges on the existence of a mass gap in these systems, namely glueball and pion respectively. On the other hand, 1+1 dimensional lattice ϕ^4 theory offers an opportunity to investigate in detail the artifacts induced by the open boundary condition as the system approaches criticality.

For extracting various observables in lattice field theories, smoothing of lattice fields is essential, in order to overcome lattice artifacts. The gradient (Wilson) flow [13–15] provides a very convenient tool for smoothing, with a rigorous mathematical underpinning. For some recent studies of gradient flow in the context of scalar theory, see Refs. [16–18]. It will be very interesting to study this in 1+1 dimensional lattice ϕ^4 theory.

II. BOUNDARY CONDITIONS AND GRADIENT FLOW

In the continuum, the Euclidean Lagrangian (density) for ϕ^4 theory is given by

$$\mathcal{L} = \frac{1}{2}\partial_\mu\phi\partial_\mu\phi \ + \ \frac{1}{2}m^2\phi^2 \ + \frac{\lambda}{4!}\phi^4. \tag{1}$$

On a periodic (on all space-time directions) lattice, the Euclidean action in 'd' space-time dimension is conventionally written as [1]

$$S = -\sum_x\sum_\mu \tilde{\phi}_x\tilde{\phi}_{x+\mu} + \left(d + \frac{m_0^2}{2}\right)\sum_x \tilde{\phi}_x^2 + \frac{\lambda_0}{4!}\sum_x \tilde{\phi}_x^4 \tag{2}$$

where all the parameters and fields have been made dimensionless by multiplying them with appropriate powers of lattice spacing 'a'.

However, in order to impose open boundary condition in the temporal direction we follow the construction of the transfer matrix. For this purpose the lattice action is written in terms of time slice action density $E(t)$ as $S = \sum_t E(t)$ and the kinetic term in temporal direction is distributed symmetrically around the time slice 't'. The details are given below.

First, with the aid of forward and backward lattice derivatives

$$\partial_\mu^f\phi = \frac{1}{a}\left(\phi_{x+\mu} - \phi_x\right) \quad \text{and} \quad \partial_\mu^b\phi = \frac{1}{a}\left(\phi_x - \phi_{x-\mu}\right) \ , \tag{3}$$

we write the symmetrized expression for kinetic term as

$$\begin{aligned}\frac{1}{2}\partial_\mu\phi\partial_\mu\phi &= \frac{1}{4}\left(\partial_\mu^f\phi\partial_\mu^f\phi + \partial_\mu^b\phi\partial_\mu^b\phi\right) \\ &= \frac{1}{4a^2}\left(\ 2\sum_\mu \phi_x^2 \ + \ \phi_{x+\mu}^2 \ + \ \phi_{x-\mu}^2 \ - \ 2\phi_x\phi_{x+\mu} \ - \ 2\phi_x\phi_{x-\mu}\right) \ .\end{aligned} \tag{4}$$

This enables one to write down the time slice action density for periodic lattice as

$$E_{\rm PBC}(t) = \mathcal{T}_t \ + \ \mathcal{V}_t \ + \ \frac{1}{2}\mathcal{T}_{t,t+1} \ + \ \frac{1}{2}\mathcal{T}_{t-1,t} \tag{5}$$

where

$$\mathcal{V}_t = \sum_{\vec{x}} \left(\frac{1}{2} a^2 m^2 \phi^2_{\vec{x},t} \; + \; \frac{a^2 \lambda}{4!} \phi^4_{\vec{x},t} \right) ,$$

$$\mathcal{T}_t \; = \; \frac{1}{4} \sum_{\vec{x},k} \Big(2 \; \phi^2_{\vec{x},t} \; + \; \phi^2_{\vec{x}+\hat{k},t} \; + \; \phi^2_{\vec{x}-\hat{k},t} \; - \; 2 \; \phi_{\vec{x},t} \; \phi_{\vec{x}+\hat{k},t} \; - \; 2 \; \phi_{\vec{x},t} \; \phi_{\vec{x}-\hat{k},t} \Big) ,$$

$$\mathcal{T}_{t,t+1} = \frac{1}{2} \sum_{\vec{x}} \Big(\phi^2_{\vec{x},t} \; + \; \phi^2_{\vec{x},t+1} \; - \; 2 \; \phi_{\vec{x},t} \; \phi_{\vec{x},t+1} \Big) ,$$

$$\mathcal{T}_{t-1,t} = \frac{1}{2} \sum_{\vec{x}} \Big(\phi^2_{\vec{x},t} \; + \; \phi^2_{\vec{x},t-1} \; - \; 2 \; \phi_{\vec{x},t} \; \phi_{\vec{x},t-1} \Big)$$

with $\hat{k}$ being the unit vector in an arbitrary spatial direction.

Following this definition, we denote $e^{-H_m(t,t+1)}$ as the general transfer matrix element between the time slices t and $t+1$ where

$$H_m \left(t, t+1 \right) = \frac{1}{2} \left(\mathcal{T}_t + \mathcal{V}_t \right) \; + \; \frac{1}{2} \left(\mathcal{T}_{t+1} + \mathcal{V}_{t+1} \right) \; + \; \mathcal{T}_{t,t+1}. \tag{6}$$

Particularly for a lattice of temporal extent 'T', the transfer matrix element between the boundary time slices $t = T-1$ and $t = 0$ is determined by

$$H_m \left(T-1, 0 \right) \; = \; \frac{1}{2} \left(\mathcal{T}_{T-1} + \mathcal{V}_{T-1} \right) \; + \; \frac{1}{2} \left(\mathcal{T}_0 + \mathcal{V}_0 \right) \; + \; \mathcal{T}_{T-1,0}$$

Now, if the temporal boundary becomes open, corresponding term drops out from the partition function. This leads us to relate the actions for lattices with two different boundary conditions in temporal direction (periodic and open) as $S_{\rm PBC} = S_{\rm OPEN} + \Delta S$ where $\Delta S = H_m \left(T-1, 0 \right)$.

The absence of the term ΔS from the action for lattice with open boundary (temporal direction), in turn, also modifies the expressions for action densities at the temporal boundaries. They are given by

$$E_{\rm OPEN}(t=0) = \frac{1}{2} \left(\mathcal{T}_0 \; + \; \mathcal{V}_0 \right) \; + \; \frac{1}{2} \mathcal{T}_{0,1} \tag{7}$$

$$\text{and} \quad E_{\rm OPEN}(t=T-1) = \frac{1}{2} \left(\mathcal{T}_{T-1} \; + \; \mathcal{V}_{T-1} \right) \; + \; \frac{1}{2} \mathcal{T}_{T-2,T-1}. \tag{8}$$

Within the bulk ($0 < t < T-1$), $E_{\rm OPEN}(t) \; = \; E_{\rm PBC}(t)$.

In order to smooth the lattice ϕ field, gradient flow is used. For ϕ^4 theory in the Euclidean space, in the continuum, the flow equation is given by

$$\begin{aligned} \frac{\partial \psi \left(x, \tau \right)}{\partial \tau} &= - \frac{\delta S \left[\psi \right]}{\delta \psi \left(x, \tau \right)} \\ &= \partial_\mu \partial_\mu \psi(x,\tau) - m^2 \psi(x,\tau) \; - \frac{\lambda}{6} \psi^3(x,\tau) \end{aligned} \tag{9}$$

where $\psi(x, \tau = 0) = \phi(x)$ with 'τ' being the flow time.

We numerically solve this equation on the lattice using the $2^{\rm nd}$ order Runge-Kutta method.

III. EXTRACTION OF BOSON MASS FROM LATTICES WITH DIFFERENT BOUNDARIES

For the extraction of boson mass we have used the simplest and the most familiar scalar operator - the time sliced field $\phi(t) = \frac{1}{V} \sum\limits_{\vec{x}} \phi \left(\vec{x}, t \right)$ where V is the spatial volume of the lattice. The mass can be easily extracted from the two point correlation function for this scalar operator which, in case of periodic boundary in temporal direction, behaves as

$$\begin{aligned} G(t) = \langle \phi(t) \phi(t=0) \rangle_{\rm PBC} &\approx C_0 \; + \; C_1 \left[e^{-mt} \; + \; e^{-m(T-t)} \right] \\ &= C_0 \; + \; 2 C_1 \; e^{-mT/2} \; \cosh m \Big(\frac{T}{2} - t \Big) \end{aligned} \tag{10}$$

where

$$C_1 = \frac{|\langle 0\,|\phi\,(0)|\,B\rangle|^2}{2m} \tag{11}$$

with $|\,B\rangle$ being the one boson state. To improve statistics, one can average over the source time as well. The effective mass can be evaluated by solving the equation $F(m) = 0$

$$\text{where} \quad F(m) \;=\; (r_1 - 1)\,\Big[\cosh m(\Delta t - 1) \;-\; \cosh m\Delta t\Big] \;+\; (1 - r_2)\,\Big[\cosh m(\Delta t + 1) \;-\; \cosh m\Delta t\Big] \tag{12}$$

$$\text{with} \quad r_1 \;=\; \frac{G(t-1)}{G(t)}, \quad r_2 \;=\; \frac{G(t+1)}{G(t)} \quad \text{and} \quad \Delta t = T/2 - t\ . \tag{13}$$

In case of open boundary in time direction, to avoid the boundary effects one needs to be well within the bulk while computing the two point correlation function. However, the second exponential will be absent from the expression of the two point function due to the loss of periodicity. On the other hand, as the time translational invariance is also lost in this case, one cannot average over the source time as well. However, within the bulk, well away from the boundary region translational invariance is recovered. So one can take average over few time slices to regain statistics.

However, this effort breaks down as one approaches the critical region. It will be shown later on in this study that, the effect of open boundary starts to engulf the whole bulk region as we move towards the critical point. Mass extraction from two point function becomes almost impossible.

Surprisingly, the open boundary itself opens up new pathways to extract the mass. Following Ref. [9], in this section we review how the boson mass can be extracted from a one-point function in open boundary using a generic time sliced scalar operator $\mathcal{O}(t)$.

We start from

$$\begin{aligned}
\langle\mathcal{O}(t)\rangle_{\rm OPEN} &= \frac{\int \mathcal{D}\phi\ \mathcal{O}(t)\ e^{-S_{\rm OPEN}}}{\int \mathcal{D}\phi\ e^{-S_{\rm OPEN}}} \\
&= \frac{\int \mathcal{D}\phi\ \mathcal{O}(t)\ e^{-S_{\rm PBC}+\Delta S}\Big/\int \mathcal{D}\phi\ e^{-S_{\rm PBC}}}{\int \mathcal{D}\phi\ e^{-S_{\rm PBC}+\Delta S}\Big/\int \mathcal{D}\phi\ e^{-S_{\rm PBC}}} \\
&= \langle\mathcal{O}(t)\rangle_{\rm PBC} \;+\; \frac{\big\langle\mathcal{O}(t)\ e^{\Delta S}\big\rangle^{\rm connected}_{\rm PBC}}{\langle e^{\Delta S}\rangle_{\rm PBC}} \qquad (14) \\
&= \langle\mathcal{O}(t)\rangle_{\rm PBC} \;+\; \frac{1}{r}\Big\langle\mathcal{O}(t)\ e^{H_m(T-1,0)}\Big\rangle^{\rm connected}_{\rm PBC} \qquad (15)
\end{aligned}$$

where $r = \langle e^{\Delta S}\rangle_{\rm PBC} = \langle e^{H_m(T-1,0)}\rangle_{\rm PBC}$. As $e^{H_m(t,t+1)}$ is also a scalar operator, from eq. 15 we have

$$\langle\mathcal{O}(t)\rangle_{\rm OPEN} \approx \langle\mathcal{O}(t)\rangle_{\rm PBC} \;+\; 2C_1'\ e^{-mT/2}\ \cosh m\Big(\frac{T}{2} - t\Big). \tag{16}$$

where m is the scalar boson mass.

Thus we find that one can extract certain two-point correlators computed with periodic boundary condition in the temporal direction by analyzing the data for the functional average of a scalar operator (one-point function) computed with open boundary (in the temporal direction) in the region of t where it differs, due to the breaking of translational invariance, from the same computed with periodic boundary. Now due to time translational invariance in the case of PBC, we can assume $\langle\mathcal{O}(t)\rangle_{\rm PBC}$ to be constant and the evaluation of effective mass can then be done again following the eqns. 12 and 13.

IV. NUMERICAL RESULTS

As we have restricted ourselves into $1+1$ dimension within this study, the fields are dimensionless here. The notations for the bare parameters of the theory on the lattice are chosen to be $m_0^2 = a^2m^2$ and $\lambda_0 = a^2\lambda$. As we know, for the stability of the theory one must have $\lambda_0 \geq 0$ and the phase transition associated with the spontaneous breaking (or restoration) of $Z(2)$ symmetry takes place only for $m_0^2 < 0$.

For the study with periodic boundary in both directions, following the method of Brower and Tamaya [19], we have used Wolff's single cluster algorithm [20, 21] blended with the standard metropolis algorithm in 1:1 ratio for

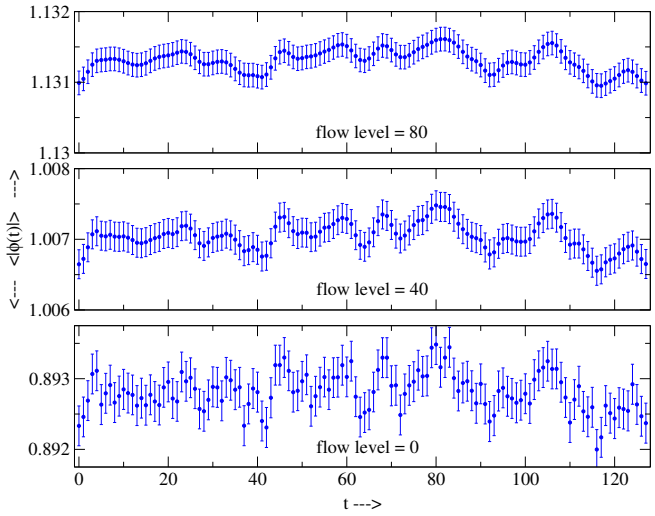

FIG. 1. Plot of expectation value of $|\phi(t)|$ for $m_0^2 = -0.5$, $\lambda_0 = 1.65$ and $L = 128$ with PBC for three different gradient flow levels.

the generation of field configurations. For the details of the whole procedure, see [1]. However, in the study with open boundary in the temporal direction (periodic in spatial direction), we resort only to the standard metropolis algorithm for configuration generation.

Following the discussions in [1], we have used $\langle|\,\phi\,|\rangle$ as the order parameter to investigate the phase structure. Here, $\phi = \sum_{\text{sites } x} \phi\,(x)\,/\text{lattice volume}$. The absolute value is taken to avoid the effect of tunnelling enforced by the algorithm of configuration generation. For the phase diagram we mainly resorted to the former study [1]. Here, we will study the effects of gradient flow and boundary conditions on the phase diagram in due course.

In this work, we explored the phase structure and the spectrum of the theory for two different sets of bare parameters given by $m_0^2 = -0.5$ and $m_0^2 = -1.0$. For each set of parameters (i.e., m_0^2 and λ_0), we have first discarded 10^6 configurations for thermalization and then generated another 10^8 configurations for the measurement purpose. Measurements are done on one in every thousand configurations. In order to study the finite size effects on the results, whole investigations have been done with four different lattice volumes such as 48^2, 64^2, 96^2 and 128^2.

Configurations chosen for measurements are placed under gradient flow which is run for one hundred steps, to be called as flow level, with a stepsize of $\delta\tau = 0.02$. Measurements are done after every ten flow levels in addition to the measurement done before the flow is started.

Now we discuss the effects of gradient flow and boundary conditions on various observables of interest. We start with the basic observable- time sliced scalar field $\phi(t)$. For the reasons stated above, here too, we take absolute value before evaluating the configuration average.

In Figs. 1 and 2, respectively for periodic and open boundary conditions in temporal directions, we present the expectation value of $|\phi(t)|$ in three different subdiagrams- one without any gradient flow and two others with two different levels of gradient flow all for a particular set of lattice parameters $m_0^2 = 0.5$, $\lambda_0 = 1.65$ and 128^2 lattice. The figures clearly show the smoothening effect with the increase of flow level. Note that, values of $\langle|\,\phi(t)\,|\rangle$ are gradually rising up with increasing flow level. The widths of windows for the values of $\langle|\phi(t)|\rangle$ are taken to be same in all the three subdiagrams instead of taking them to be proportional to the respective average values. This actually has reduced the manifestation of smoothening effect to some extent.

To make exhibition of boundary effect clearer, in Fig. 3, we compare the behaviour of $\langle|\,\phi(t)\,|\rangle$ for $m_0^2 = -0.5$ and $L = 128$ for periodic and open boundary conditions without any gradient flow for three different values of λ_0 all in the broken symmetric phase. For the smallest value of the coupling which is far away from the critical point, effects of open boundary are found to be only at the edges leaving a long bulk region matching with the counterpart in PBC. As the coupling increases one gets closer to the region of phase transition and effect of open boundary extends on both side squeezing the bulk. For $\lambda_0 = 1.86$, we are already in the critical region and we observe that the bulk region is almost vanished. The same is presented in Fig. 4 for gradient flow level 50. We notice that it only smoothens the data (which is, although, hardly visible here because of the wide scale of values for $\langle|\,\phi(t)\,|\rangle$ covered in the figure) leaving the boundary effects unchanged.

In Fig. 5 we plot $\langle|\,\phi\,|\rangle$ versus λ_0 for different values of the gradient flow level for 128^2 lattice at $m_0^2 = -0.5$. The

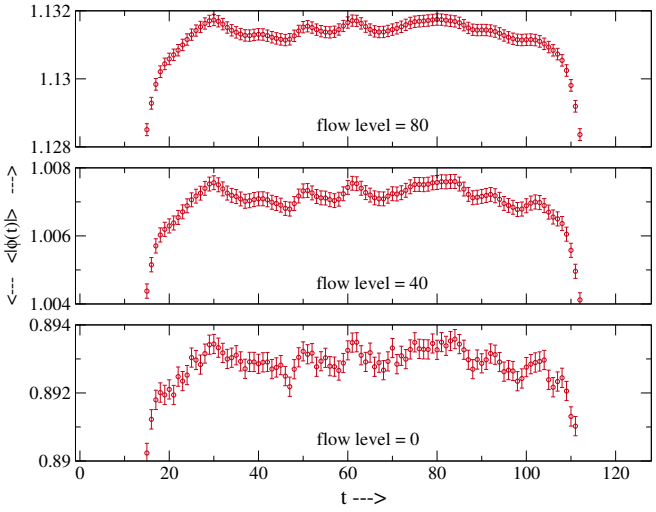

FIG. 2. Plot of expectation value of $|\phi(t)|$ for $m_0^2 = -0.5$, $\lambda_0 = 1.65$ and $L = 128$ with OPEN for three different levels of gradient flow.

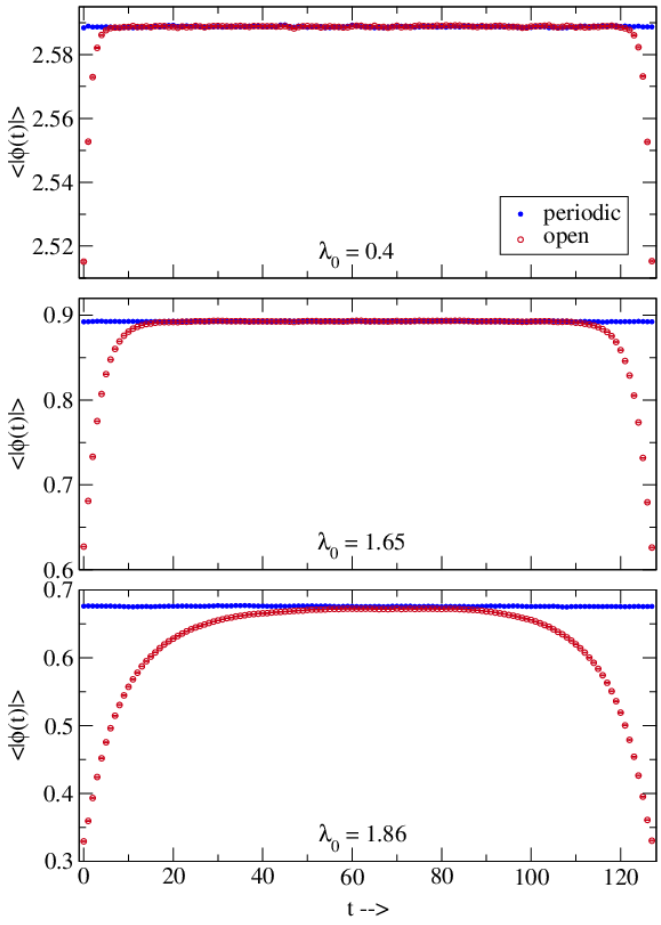

FIG. 3. Comparison of $\langle|\phi(t)|\rangle$ between PBC and OPEN for $m_0^2 = -0.5$, $L = 128$ and three different values of λ_0 without any gradient flow.

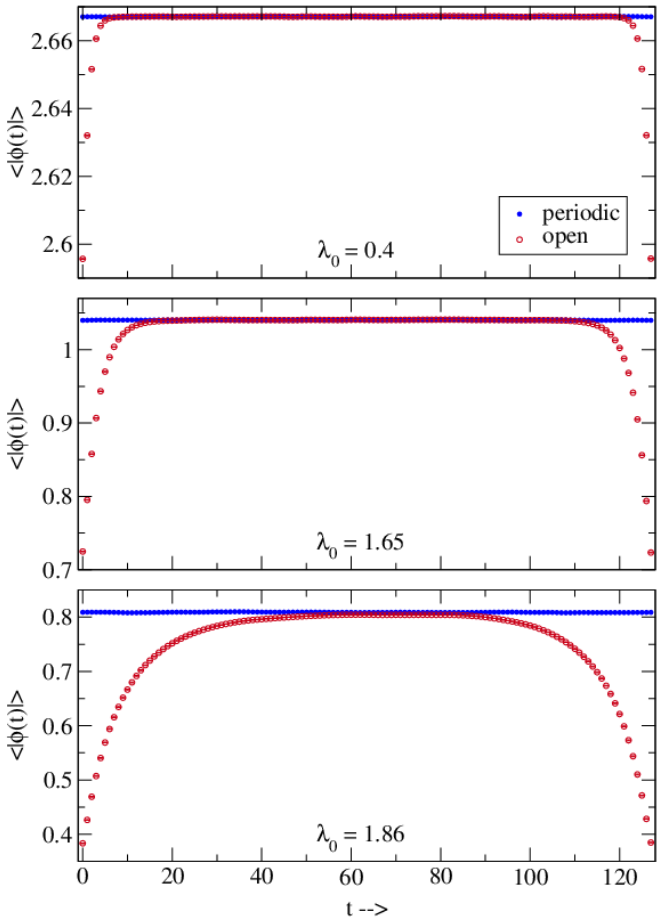

FIG. 4. Comparison of $\langle|\phi(t)|\rangle$ between PBC and OPEN for $m_0^2 = -0.5$, $L = 128$ and three different values of λ_0 at gradient flow level 50.

monotonous rise in the value of $\langle|\,\phi\,|\rangle$ with increasing gradient flow level is consistent with the behaviour of $\langle|\,\phi(t)\,|\rangle$. Details of the behavior in the critical region are shown in the inset of the figure. The trend is seemed to be retained across the phase transition.

In Fig. 6, we present the comparison between $\langle|\,\phi\,|\rangle$ computed using PBC and the same obtained with OPEN for different lattice sizes at $m_0^2 = -0.5$ before applying the gradient flow on the fields. Deep in both the broken-symmetric and the symmetric phases, for all the lattice volumes, the results for PBC and OPEN are found to be matching within our statistical error. However, inside the critical region a clear disagreement is observed. Phase transition appears to take place at smaller values of λ_0 in case of OPEN compared to PBC. However, the gap between the transition point in two different boundaries seems to be vanishing with the increase of lattice size. This behavior is consistent with the expectation that the effect of boundary surface diminishes in infinite volume limit. The picture remains to be almost unaltered by the application of gradient flow other than raising the values universally little bit. This has been emphasized in Fig. 7.

Now we study the effects of gradient flow and the boundary conditions on the behaviour of another observable of interest, susceptibility $\chi = \sum_x \langle\phi(x)\phi(0)\rangle$/lattice volume. In Fig. 8, we show the behaviour of susceptibility as a function of λ_0 for $m_0^2 = -0.5$ with PBC on 128^2 lattice for different levels of gradient flow. Consistent with the trends as observed in case of $\langle|\,\phi\,|\rangle$, the peak of susceptibility becomes higher and higher as the level of gradient flow increases leaving the peak position unchanged.

Analogous to the study done for $\langle|\,\phi\,|$, we compare the susceptibility between periodic and open boundary conditions for different lattice sizes (L) at $m_0^2 = -0.5$ and gradient flow level 50 in Fig. 9. Here too, we observe that compared to the case of PBC, the peak is shifted towards the smaller values of λ_0 in case of OPEN at a fixed L and the magnitude of the shift decreases as L increases.

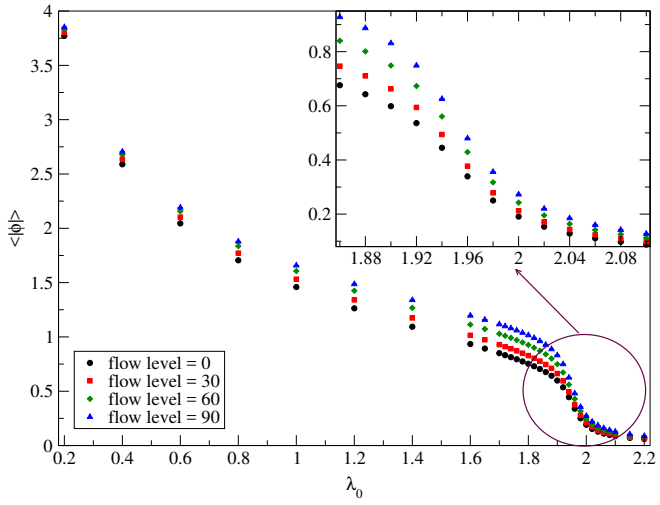

FIG. 5. Plot of $\langle|\phi|\rangle$ versus λ_0 for different values of the gradient flow level for $m_0^2 = -0.5$ and $L = 128$ in case of PBC.

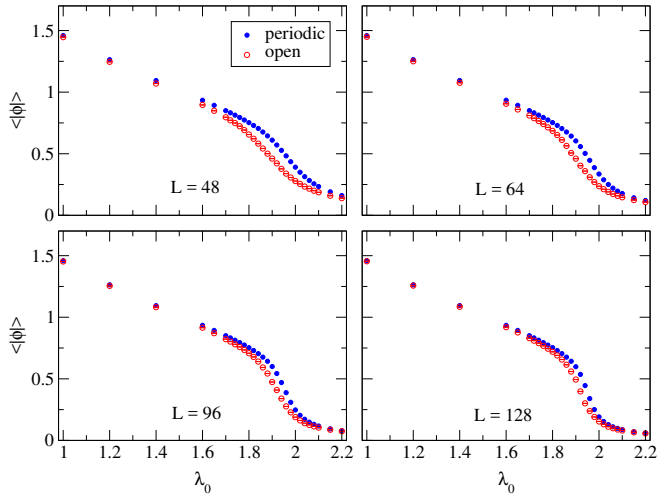

FIG. 6. Plot of $\langle|\phi|\rangle$ versus λ_0 for PBC and OPEN without gradient flow for different L at $m_0^2 = -0.5$.

This shift in the peak position of susceptibility between PBC and OPEN seems to be unaffected by gradient flow as per our expectation. This has been demonstrated in Figs. 10 and 11 for the smallest and largest lattices sizes $L = 48$ and $L = 128$ respectively both with $m_0^2 = -0.5$.

The fact that the value of $\langle|\phi|\rangle$ changes with gradient flow even in the critical region raises an interesting question. Does the determination of critical coupling in a finite size scaling (FSS) analysis gets affected by gradient flow? Here we study the possible effect of gradient flow in the FSS of the data for $\langle|\phi|\rangle$ to determine the critical coupling. We follow the discussion of the main aspects of Finite Size Scaling [22–24] given in Ref. [1]. FSS assumes that, in a finite system, out of the three length scales involved, namely, the correlation length ξ, the size of the system L and the microscopic length a (lattice spacing), the last one drops out near the critical region due to universality.

For any observable P_L computed on a lattice of finite extent L, the nonanaliticity near the critical point in the infinite volume limit can be expressed in the form of a scaling law $P_\infty(\tau) = A_P \tau^{-\rho}$ where $\tau = (\lambda_0^c - \lambda_0)/\lambda_0^c$ and ρ is the critical exponent associated with the observable. Following the arguments of FSS analysis, it can be shown that

$$L^{\rho/\nu}/P_L(\tau) = A_P^{-1}\, A_\xi^{\rho/\nu}\, \left[\mathrm{C_P} + \mathrm{D_P}\, A_\xi^{-1/\nu}\, \tau\, L^{1/\nu} + \mathcal{O}(\tau^2)\right] \tag{17}$$

where ν is the critical exponent associated with the correlation length ξ. Eq. (17) implies that if we plot $L^{\rho/\nu}/P_L\,(\tau)$

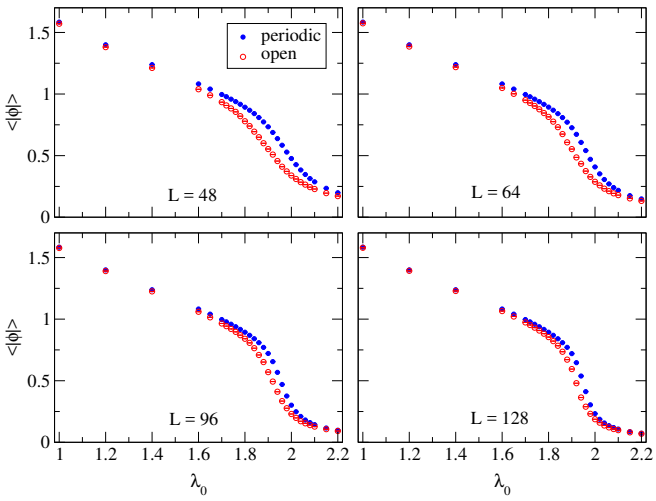

FIG. 7. Plot of $\langle|\phi|\rangle$ versus λ_0 for PBC and OPEN at gradient flow level 50 for different L at $m_0^2 = -0.5$.

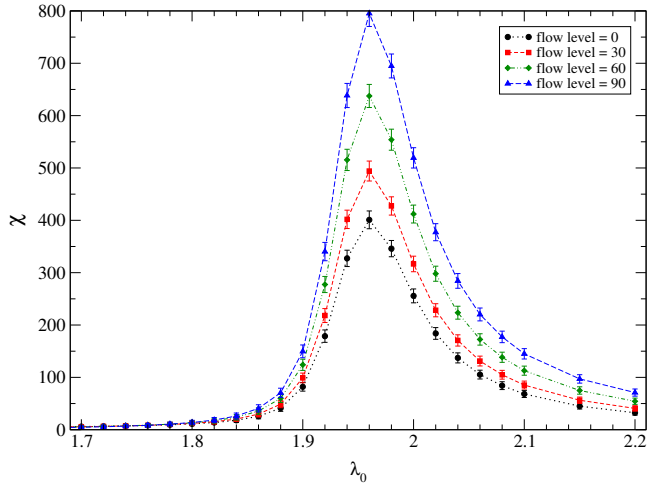

FIG. 8. Comparison of susceptibility for different levels of gradient flow with PBC at $m_0^2 = -0.5$ and $L = 128$.

versus the coupling λ_0 for different values of L, all the curves will pass through the same point where $\tau = 0$ or equivalently $\lambda_0 = \lambda_0^c$ [24].

The critical behavior of $\langle\phi\rangle$, the susceptibility χ and the mass gap $m = 1/\xi$ may be written as

$$\langle\phi\rangle \;=\; A_\phi^{-1}\,\tau^\beta, \quad \chi \;=\; A_\chi\,\tau^{-\gamma} \quad \text{and} \quad m \;=\; A_\xi^{-1}\,\tau^\nu. \tag{18}$$

From the general expectation that in $1+1$ dimensions, ϕ^4 theory and Ising model belong to the same universality class, we have used the Ising values for the corresponding exponents as inputs in our FSS analysis. Thus, $\beta = 0.125$, $\gamma = 1.75$ and $\nu = 1$.

The plot of $\langle|\phi|\rangle L^{0.125}$ versus λ_0 for different values of the gradient flow level at $m_0^2 = -0.5$ with periodic boundary in the temporal direction is presented in Fig. 12. In spite of the fact that $\langle|\phi|\rangle$ changes with gradient flow level, the critical coupling λ_0^c is found to be unaffected by gradient flow. The critical coupling λ_0^c is found to be little less than 1.94 for $m_0^2 = -0.5$. Similar FSS analysis has been done at $m_0^2 = -1.0$ leading to the same conclusion along with an estimated value of $\lambda_0^c \approx 4.46$.

A similar FSS analysis of the susceptibility calculated at $m_0^2 = -0.5$ for various values of gradient flow level (for PBC) is presented in Fig. 13. Here, the smoothening effect of gradient flow has helped to pinpoint the location of critical coupling λ_0^c which matches with the estimation done from the FSS analysis for $\langle|\phi|\rangle$. Similar FSS analysis

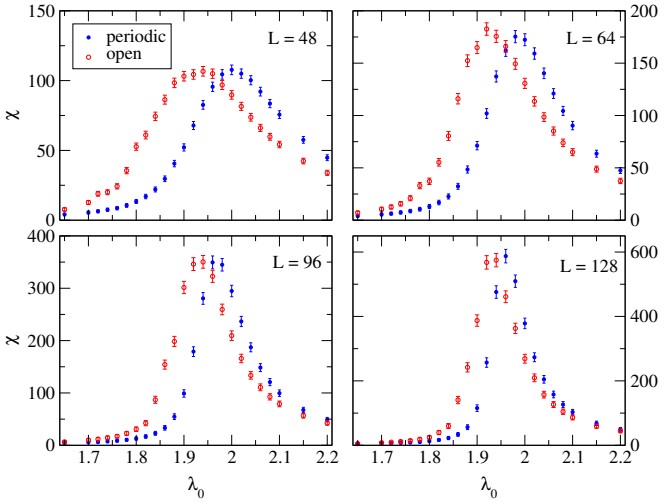

FIG. 9. Comparison of susceptibility between PBC and OPEN for different L at $m_0^2 = -0.5$ and gradient flow level 50.

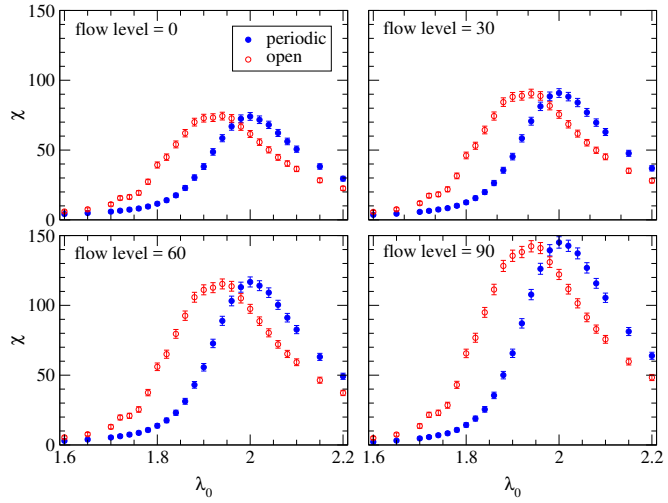

FIG. 10. Comparison of susceptibility between PBC and OPEN for different levels of gradient flow at $m_0^2 = -0.5$ with $L = 48$.

done at $m_0^2 = -1.0$ also gives the corresponding value of λ_0^c matching with the same obtained from FSS analysis for $\langle|\phi|\rangle$.

Using the same ansatz, we have tried an FSS analysis for both $\langle|\phi|\rangle$ and χ in case of open boundary in temporal direction. The results are respectively presented in Figs. 14 and 15. It is obvious from the figures that the critical point is not pinpointed that clearly like in the case of PBC. A strange pattern is found for susceptibility for which the curves with different L, instead of passing through a point, appear to overlap within statistical errors at and between the values 1.92 and 1.94 of λ_0. Anyway, the effect of surface in case of open boundary needs to be taken into the ansatz for finite size scaling analysis. For that purpose a more precise numerical study is necessary which is beyond the scope of this study.

Finally, we present the results for the mass spectrum of the theory. The boson mass has been extracted from the plateau along time direction for effective mass which is computed from two point and one point correlation function of the time sliced scalar field $\phi(t)$ respectively for PBC and OPEN. For this purpose, we first find out the gradient flow level for which the plateau for effective mass is found to be the most stable one separately for each coupling (also for PBC and OPEN separately). The computation of mass has been done only for the two largest lattices namely for $L = 96$ and $L = 128$ as for the smaller lattices, the temporal extent is not sufficiently long to get the fall of correlation function particularly within the critical region. Because of this, it is not meaningful to perform the formal

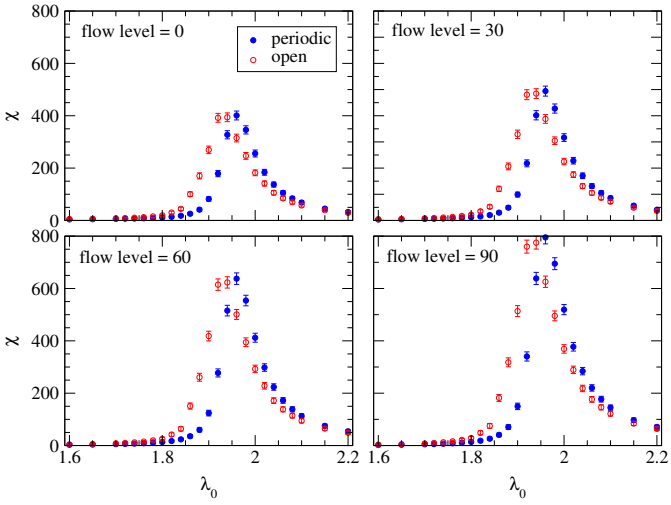

FIG. 11. Comparison of susceptibility between PBC and OPEN for different levels of gradient flow at $m_0^2 = -0.5$ with $L = 128$.

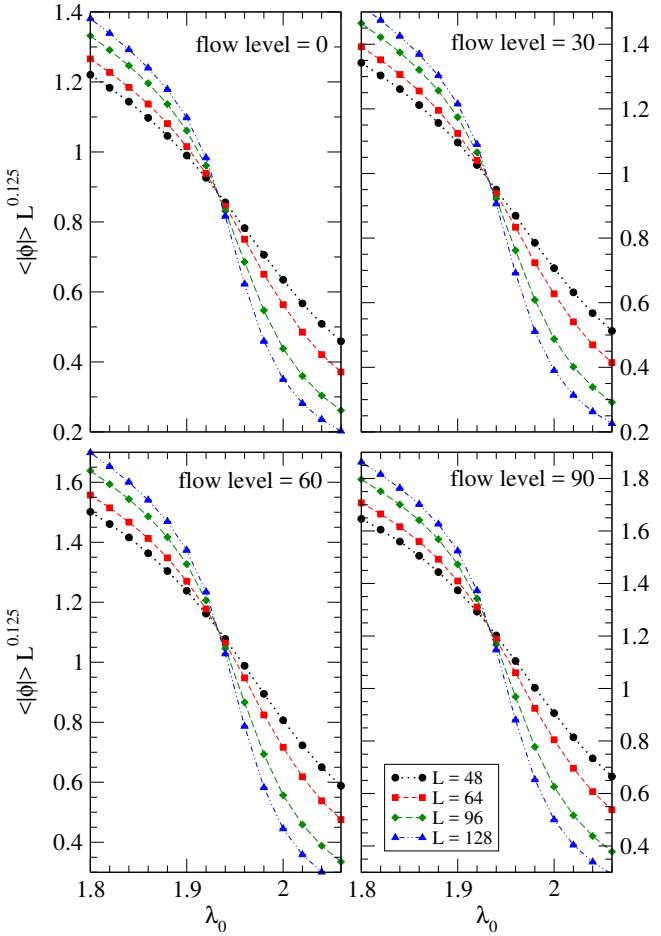

FIG. 12. Plot of $\langle|\phi|\rangle L^{0.125}$ versus λ_0 for different levels of gradient flow with PBC at $m_0^2 = -0.5$.

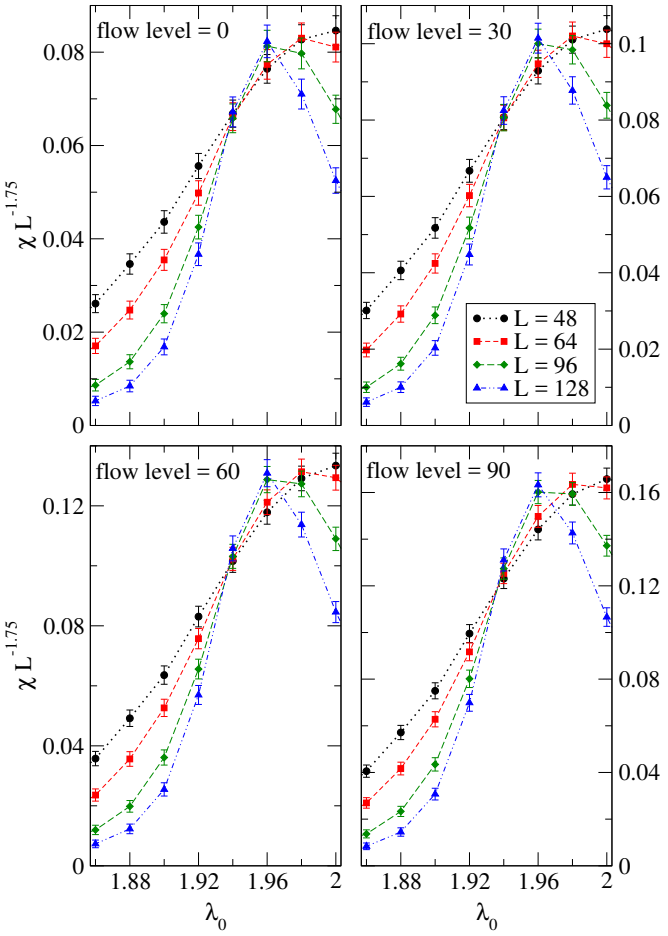

FIG. 13. Plot of $\chi L^{-1.75}$ versus λ_0 for different levels of gradient flow with PBC at $m_0^2 = -0.5$.

FSS analysis. However, even with lattices of only two different sizes, we observe noticeable finite volume effect.

In Figs. 16 and 17 we compare the volume dependence of the boson mass versus λ_0 for periodic (top) and open (bottom) at $m_0^2 = -0.5$ and $m_0^2 = -1.0$ respectively. In case of PBC, the effect of finite volume on the mass spectrum is clearly visible in the critical region. Although for OPEN, this effect is not that obvious from the respective figure. However, if we remember from the behaviors of $\langle|\phi|\rangle$ and χ that the phase transition point shifts towards the smaller values of λ_0 compared to PBC and that the shift is more for smaller volume, it appears that this leftward shift of transition point has overshadowed the finite volume effect.

The effects of the boundary on the mass spectrum have been demonstrated in Figs. 18 and 19 respectively for two different values for lattice mass parameters $m_0^2 = -0.5$ and $m_0^2 = -1.0$ respectively. The leftward shift of the phase transition point is found to be almost diminishing for the larger lattice. The boundary effects are more prominent near the critical point.

V. CONCLUSIONS

We have found gradient flow to be very effective in reducing the unwanted lattice artifacts in the functional average of the time sliced field $\phi(t)$ and in the extraction of boson mass from both two-point (PBC) and one-point (OPEN) correlators. We have shown that, in spite of the fact that $\langle|\phi|\rangle$ changes with gradient flow, the critical value of λ_0 does not depend on the gradient flow level. In the case of susceptibility, it is found that the increase in the level of gradient flow raises the height of the peak but leaves the peak position (phase transition point for a given volume) unaltered. Critical coupling λ_0^c has been obtained for both $\langle|\phi|\rangle$ and χ from a detailed finite size scaling analysis of the data for various lattice sizes and gradient flow levels with results unchanged with flow level. With open boundary

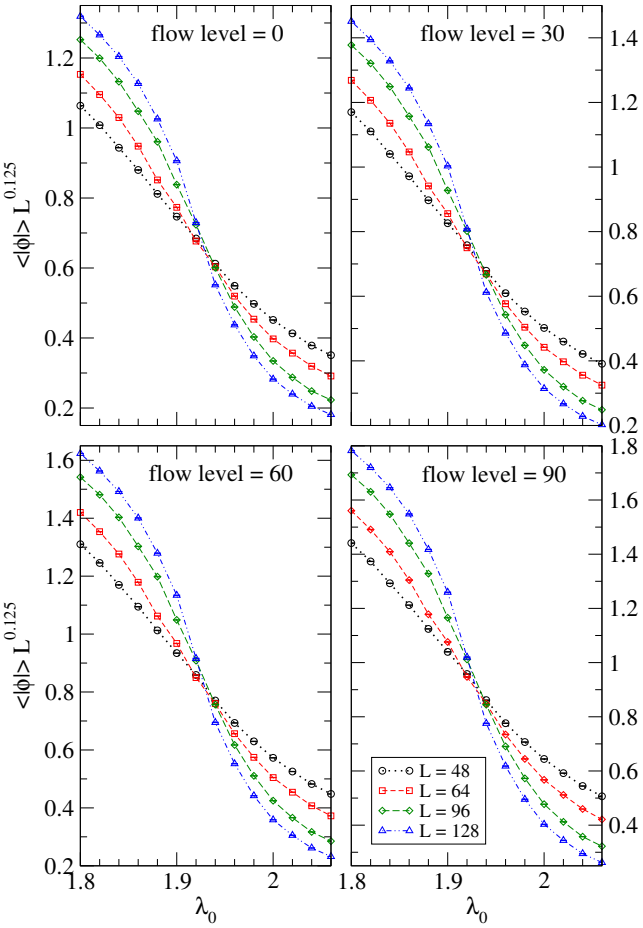

FIG. 14. Plot of $\langle|\phi|\rangle L^{0.125}$ versus λ_0 for different levels of gradient flow at $m_0^2 = -0.5$ with open boundary.

condition in the temporal direction, one can extract the boson mass by studying the one-point function of $\phi(t)$ which we have compared with that extracted from the two-point function in the case of periodic boundary condition. We observe noticeable boundary effects on the mass spectrum in the critical region where the boundary artifacts extend deeply in to the bulk region and the finite volume artifacts become much more important compared to the case of periodic boundary condition. An extensive analytical study of the boundary effects due to open boundary in the critical region, taking in to consideration finite size scaling will be very fruitful.

ACKNOWLEDGMENTS

To carry out all the numerical calculations reported in this work, Cray XE6 system supported by the 11th-12th Five Year Plan Projects of the Theory Division, SINP under the Department of Atomic Energy, Govt. of India, is used. We thank Richard Chang for the prompt maintenance of the system.

[1] A. K. De, A. Harindranath, J. Maiti and T. Sinha, *Investigations in 1+1 dimensional lattice ϕ^4 theory*, Phys. Rev. D **72**, 094503 (2005) doi:10.1103/PhysRevD.72.094503 [hep-lat/0506002].

[2] A. K. De, A. Harindranath, J. Maiti and T. Sinha, *Topological charge in 1+1 dimensional lattice ϕ^4 theory*, Phys. Rev. D **72**, 094504 (2005) doi:10.1103/PhysRevD.72.094504 [hep-lat/0506003].

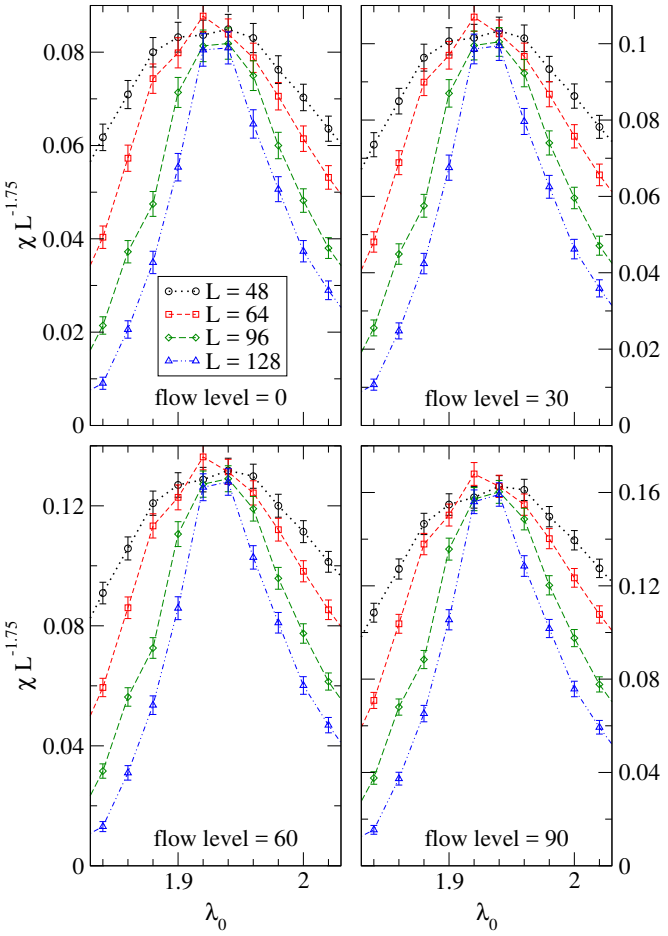

FIG. 15. Plot of $\chi L^{-1.75}$ versus λ_0 for different levels of gradient flow at $m_0^2 = -0.5$ with open boundary.

[3] M. Lüscher, *Topology, the Wilson flow and the HMC algorithm*, PoS LATTICE **2010**, 015 (2010) [arXiv:1009.5877 [hep-lat]].

[4] M. Lüscher and S. Schaefer, *Lattice QCD without topology barriers*, JHEP **1107**, 036 (2011) [arXiv:1105.4749 [hep-lat]].

[5] M. Lüscher and S. Schaefer, *Lattice QCD with open boundary conditions and twisted-mass reweighting*, Comput. Phys. Commun. **184**, 519 (2013) [arXiv:1206.2809 [hep-lat]].

[6] A. Chowdhury, A. Harindranath, J. Maiti and P. Majumdar, *Topological susceptibility in lattice Yang-Mills theory with open boundary condition*, JHEP **02**, 045 (2014) [arXiv:1311.6599 [hep-lat]].

[7] A. Chowdhury, A. Harindranath and J. Maiti, *Open Boundary Condition, Wilson Flow and the Scalar Glueball Mass*, JHEP **1406**, 067 (2014) [arXiv:1402.7138 [hep-lat]].

[8] A. Chowdhury, A. Harindranath and J. Maiti, *Correlation and localization properties of topological charge density and the pseudoscalar glueball mass in SU(3) lattice Yang-Mills theory*, Phys. Rev. D **91**, 074507 (2015) [arXiv:1409.6459 [hep-lat]].

[9] A. Chowdhury, A. Harindranath and J. Maiti, *Physical observables from boundary artifacts: scalar glueball in Yang-Mills theory*, JHEP **1602**, 134 (2016) [arXiv:1509.07959 [hep-lat]].

[10] A. Amato, G. Bali and B. Lucini, *Topology and glueballs in $SU(7)$ Yang-Mills with open boundary conditions*, PoS LATTICE **2015**, 292 (2016) [arXiv:1512.00806 [hep-lat]].

[11] M. Bruno *et al.*, *Simulation of QCD with $N_f = 2 + 1$ flavors of non-perturbatively improved Wilson fermions*, JHEP **1502**, 043 (2015) [arXiv:1411.3982 [hep-lat]].

[12] See, for example, N. Shibata and C. Hotta, *Boundary effects in the density-matrix renormalization group calculation*, Phys. Rev. B **84**, 115116 (2011) [arXiv:1106.6202].

[13] M. Lüscher, *Trivializing maps, the Wilson flow and the HMC algorithm*, Commun. Math. Phys. **293**, 899 (2010) [arXiv:0907.5491 [hep-lat]].

[14] M. Lüscher, *Properties and uses of the Wilson flow in lattice QCD*, JHEP **1008**, 071 (2010) [arXiv:1006.4518 [hep-lat]].

[15] M. Lüscher and P. Weisz, *Perturbative analysis of the gradient flow in non-abelian gauge theories*, JHEP **1102**, 051 (2011) [arXiv:1101.0963 [hep-th]].

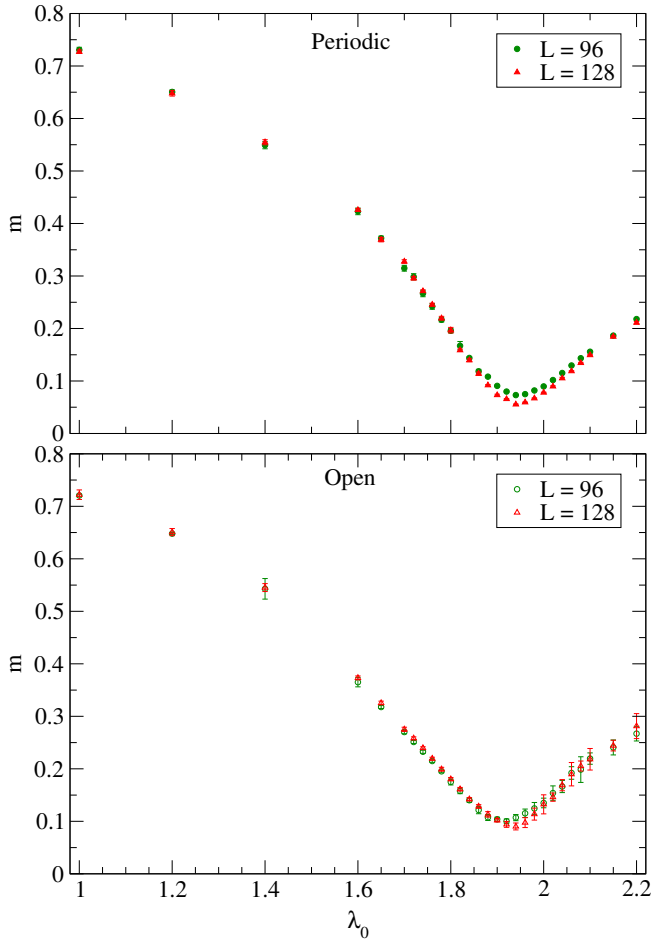

FIG. 16. The volume dependence of the boson mass versus λ_0 for PBC (top) and OPEN (bottom) at $m_0^2 = -0.5$.

[16] K. Fujikawa, *The gradient flow in $\lambda\phi^4$ theory*, JHEP **1603**, 021 (2016) doi:10.1007/JHEP03(2016)021 [arXiv:1601.01578 [hep-lat]].

[17] M. Dalla Brida, M. Garofalo and A. D. Kennedy, *Numerical Stochastic Perturbation Theory and Gradient Flow in ϕ^4 Theory*, PoS LATTICE **2015**, 309 (2016) [arXiv:1512.08222 [hep-lat]].

[18] C. Monahan, *The gradient flow in simple field theories*, PoS LATTICE **2015**, 052 (2016) [arXiv:1512.00294 [hep-lat]].

[19] R. C. Brower and P. Tamayo, Phys. Rev. Lett. **62**, 1087 (1989).

[20] U. Wolff, Int. J. Mod. Phys. C **4** 451 (1993), [arXiv:hep-lat/9209005].

[21] U. Wolff, Phys. Rev. Lett. **62**, 361 (1989).

[22] J. L. Cardy in *Finite-Size Scaling*, edited by J. L. Cardy, (Elsevier-Science Publishers, B.V., Amsterdam, 1988).

[23] E. Brézin, J. Phys. (France) **43**, 15 (1982); reprinted in Ref. [22].

[24] N. Goldenfeld, *Lectures on Phase Transitions and the Renormalization Group*, (Addison-Wesley Publishing Company, Reading, Massachusetts, 1992).

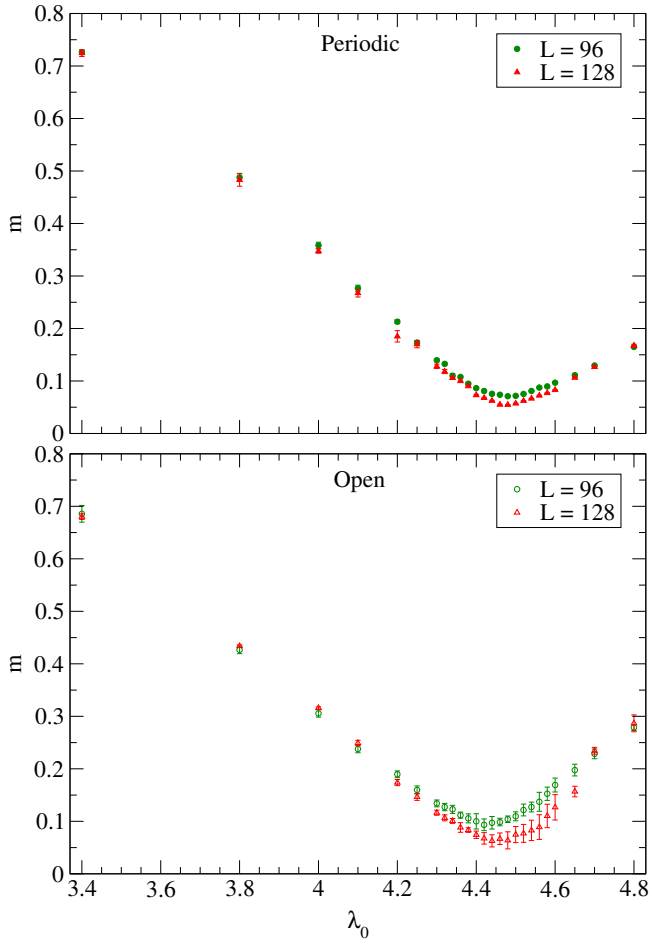

FIG. 17. The volume dependence of the boson mass versus λ_0 for PBC (top) and OPEN (bottom) at $m_0^2 = -1.0$.

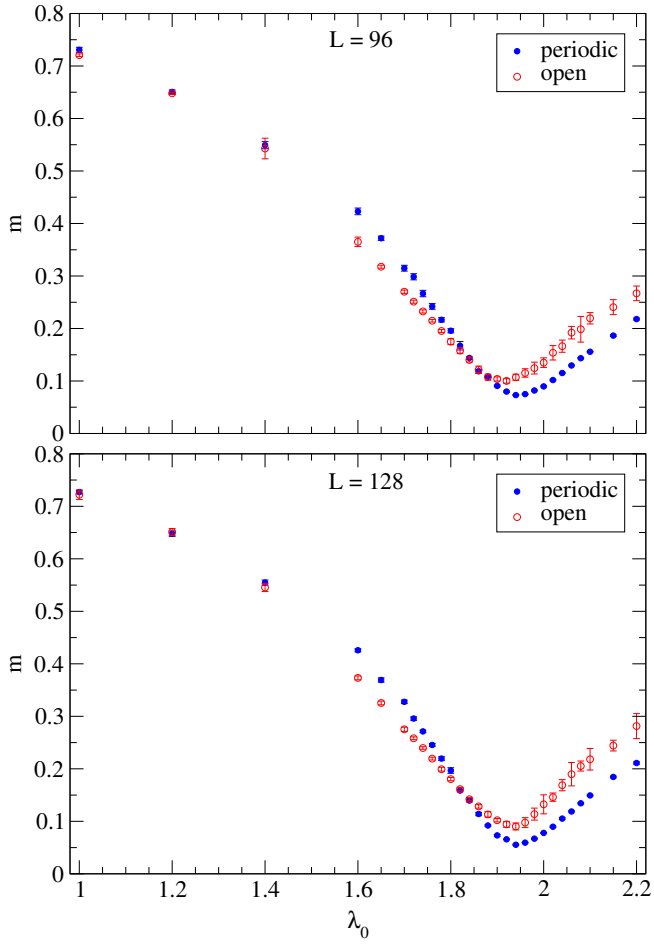

FIG. 18. The effect of boundary condition on the boson mass versus λ_0 for L=96 (top) and L=128 (bottom) at $m_0^2 = -0.5$.

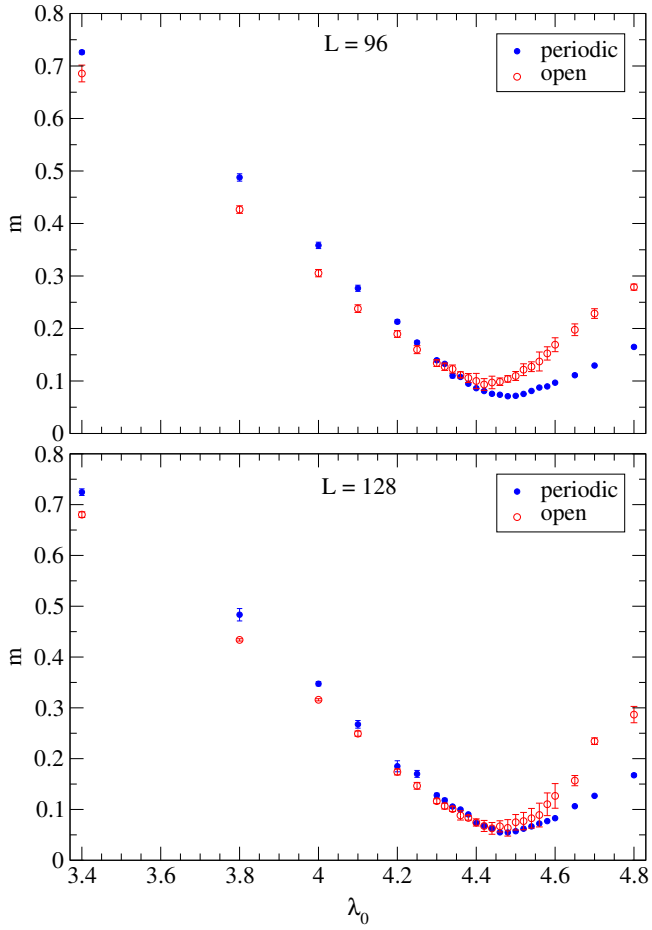

FIG. 19. The effect of boundary condition on the boson mass versus λ_0 for L=96 (top) and L=128 (bottom) at $m_0^2 = -1.0$.